Int. J. Solids Structures, 1971, Vol. 7, pp. 11 to 23. Pergamon Press. Printed in Great Britain

FINITE ELEMENT APPLICATIONS IN THE CHARACTERIZATION OF ELASTIC SOLIDS†

KENNETH T. KAVANAGH‡

Sandia Laboratories, Albuquerque, New Mexico

and

RAY W. CLOUGH§

University of California, Berkeley

Abstract—A finite element formulation of the minimum potential energy theorem is used to establish the basis for an experimental test program in composite and non-composite materials. The flexibility of the variational technique permits the experimental program to incorporate specimens of arbitrary geometry with a wide variety of stress and kinematic boundary conditions.

The resulting experimental program utilizes comparisons between mathematical results and experimental measurements to evaluate the analytical accuracy of resulting approximate mechanical descriptions.

INTRODUCTION

SUBSEQUENT to its introduction in 1956 [1], the finite element technique has developed into one of the most versatile methods for the analysis of stress and deformation in solid continua. Extensions of the basic variational principle have found application in the areas of plane stress, plate bending and shell analysis, including such behavioral effects as buckling and finite deformations, linear, nonlinear, inelastic and time-dependent materials. All such analyses implicitly assume that the material properties are known *a priori*, and that the corresponding mechanical descriptions are sufficiently accurate to justify refined mathematical solutions.

It is significant that the aerospace industry, a traditional outlet for such sophisticated analyses, is currently committed to the investigation of non-conventional materials for application in efficient, light-weight designs. These materials, notably epoxies, fiberglasses, elastomers and filamentary and particulate composites, are frequently utilized in working components after only rudimentary investigations of material behavior. Rapidly increasing use and development of such materials underscores the pressing need for material characterization techniques which are compatible in accuracy with the currently employed analytical methods.

The present paper examines an application of the finite element method in the mechanical characterization of elastic solids. The numerical technique is generally applicable to the experimental investigation of macroscopically homogeneous, time-independent materials

† This work was supported by the United States Atomic Energy Commission.

‡ Staff Member.

§ Professor of Civil Engineering, Division of Structural Engineering and Structural Mechanics.

utilizing: (1) specimen configurations with kinematic boundary restraints (as opposed to stress boundary conditions), (2) arbitrary specimen geometries and deformation modes, and (3) the inclusion of general anisotropic linear, piecewise linear and nonlinear material properties. The emphasis in the method is directed towards: (1) a consistent degree of accuracy between the analysis and the experiment, and (2) the incorporation of internal checks for the accuracy of the resultant material constants.

BACKGROUND

An examination of contemporary experimental techniques indicates that a majority of experiments are designed to approximate a specimen configuration in which the stress state is statically determinate. The slender tension specimen and the thin-walled tube have been extensively employed, since an application of St. Venants principle is sufficient to eliminate boundary effects from the stress analysis. Tubes and slender rods, however, are not applicable to all materials, and for composites in particular, flat sheet specimens have been adopted [2, 3].

Reference [2] provides an insight into errors that arise from introducing approximations in the stress analysis of two-dimensional experimental specimens. The specimen (Fig. 1) was analyzed in Ref. [2] as a stress boundary-value problem, in which the loads were approximated by a uniform stress distribution at infinity. The resultant airy stress function solution predicted a uniform state of stress at a radius (R) about the center of the specimen which will exist independent of the material properties. A finite element solution of the same problem (Fig. 2) reveals that the Airy stress function can be in error by as much as

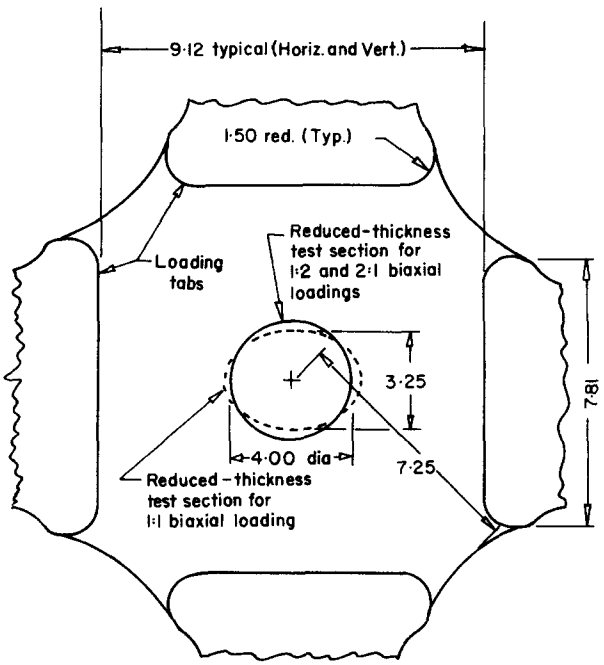

FIG. 1. Biaxial-loading specimens designs. All dimensions are in inches. (Reproduced from Ref. [2].)

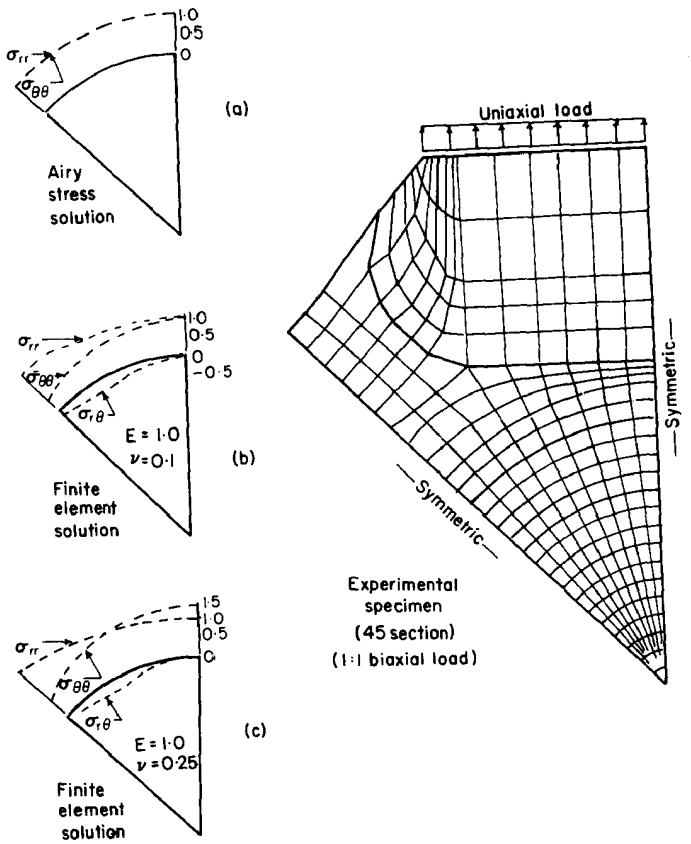

FIG. 2. Finite element analysis.

20 per cent, and that the state of stress is not independent of the material properties as assumed by the author.

The approach to be employed in this investigation emphasizes that the experiment and the analysis be carried out simultaneously. From the diagram below, it may be seen that both the experiment and the analysis form an integral part of the material characterization.

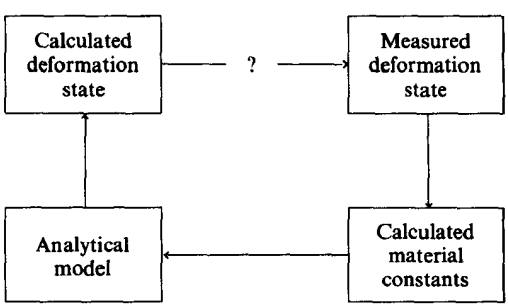

The experimental measurements are used to evaluate material constants, which are, in turn, the basis for an equivalent mathematical model. The mathematical model serves primarily as a check on the derivation of the material constants—by predicting the experimentally measured deformation state. Whenever the mathematical results coincide with the experiment, the analysis of material constants may be assumed to be correct and the characterization is complete.† A similar comparison of experiment and analysis was recently employed by Karnes [4] to illustrate errors in the analysis and assumed stress states of bar impact experiments.

For the consideration of linear materials, or for piecewise-linear increments, the experimental program can be based upon a systematic recycling of the process given above. An initial set of material properties is assumed, which can be used to predict certain characteristics of the mathematical solution. The prediction is then combined with experimental measurements to produce a "corrected" set of material constants, which becomes the basis for a new cycle. The cycle below:

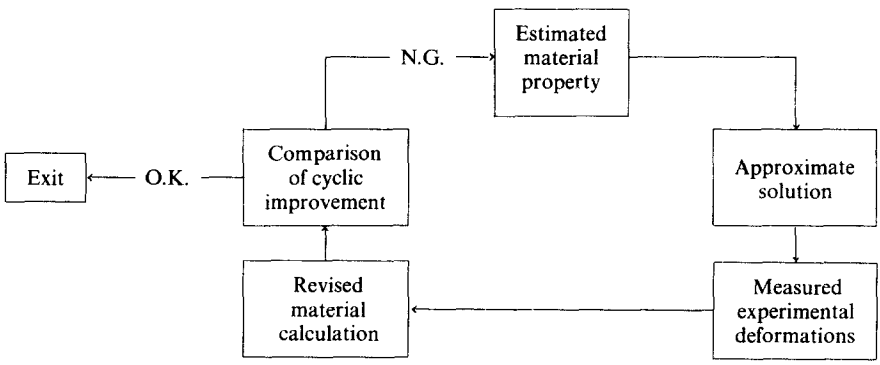

terminates whenever the predicted and corrected material constants coincide—or when successive cycles fail to produce further improvement. The failure of any cyclic improvement after (N) cycles is indicative of the error that will be incorporated in any mathematical model—and can be considered the limit of accuracy in any subsequent analysis.

ANALYTICAL PROCEDURE

The finite element background is given for a quadrilateral plane stress element, although the general procedure is applicable to plate bending, shell and three-dimensional analyses. Simple bi-linear displacement functions are assumed, and the element is developed according to a procedure by Irons [6].

Displacement functions are selected such that:

$$u = \sum_{1}^{4} \varphi_i(a, b) \, . \, u_i$$
$$v = \sum_{1}^{4} \varphi_i(a, b) \, . \, v_i \qquad (1)$$

† When comparisons are limited to a small number of data points, the question of uniqueness arises. It has been found, however, that multiple solutions will rarely occur within the limitations of positive-definite material descriptions (stable materials), and that extraneous solutions can be eliminated from physical intuition.

where:

$$u_i = \text{displacement at node } (i) \text{ in direction } (X)$$

$$v_i = \text{displacement at node } (i) \text{ in direction } (Y)$$

The functions, φ_i, are the Lagrange interpolation functions for the non-dimensional coordinates (a, b). Coordinates (a, b) are related to the global (X, Y) system through the transformation:

$$\begin{aligned} X &= \sum^{4} \varphi_i(a, b) \, . \, X_i \\ Y &= \sum^{4} \varphi_i(a, b) Y_i . \end{aligned} \tag{2}$$

Element strains are defined in terms of u_i, v_i, φ_i by:

$$\begin{aligned} \varepsilon_{xx} &= \frac{\partial u}{\partial x} = \frac{\partial}{\partial x}\{\sum \varphi_i u_i\} = \frac{\partial}{\partial a}\{\sum \varphi_i u_i\}\frac{\partial a}{\partial x} + \frac{\partial}{\partial b}\{\sum \varphi_i u_i\}\frac{\partial b}{\partial x} \\ \varepsilon_{yy} &= \frac{\partial v}{\partial y} = \frac{\partial}{\partial y}\{\sum \varphi_i v_i\} = \frac{\partial}{\partial a}\{\sum \varphi_i v_i\}\frac{\partial a}{\partial y} + \frac{\partial}{\partial b}\{\sum \varphi_i v_i\}\frac{\partial b}{\partial y} \end{aligned} \tag{3}$$

$$2\varepsilon_{xy} = \frac{\partial u}{\partial y} + \frac{\partial v}{\partial x} = \ldots = \frac{\partial}{\partial a}\{\sum \varphi_i u_i\}\frac{\partial a}{\partial y} + \frac{\partial}{\partial b}\{\sum \varphi_i u_i\}\frac{\partial b}{\partial y} + \frac{\partial}{\partial a}\{\sum \varphi_i v_i\}\frac{\partial a}{\partial x} + \frac{\partial}{\partial b}\{\sum \varphi_i v_i\}\frac{\partial b}{\partial x}$$

and subsequently converted to matrix form:

$$\begin{bmatrix} a_{,x} & b_{,x} \\ a_{,y} & b_{,y} \end{bmatrix} = \begin{bmatrix} x_{,a} & x_{,b} \\ y_{,a} & y_{,b} \end{bmatrix}^{-1} = \left\{ \begin{bmatrix} \varphi_{1,a} & \cdots & \varphi_{4,a} \\ \varphi_{1,b} & \cdots & \varphi_{4,b} \end{bmatrix} \begin{bmatrix} x_1 & y_1 \\ \vdots & \vdots \\ x_4 & y_4 \end{bmatrix} \right\} \tag{4}$$

$$\begin{bmatrix} \varphi_{1,x} & \cdots & \varphi_{4,x} \\ \varphi_{1,y} & \cdots & \varphi_{4,y} \end{bmatrix} = \begin{bmatrix} a_{,x} & b_{,x} \\ a_{,y} & b_{,y} \end{bmatrix} \begin{bmatrix} \varphi_{1,a} & \cdots & \varphi_{4,a} \\ \varphi_{1,b} & \cdots & \varphi_{4,b} \end{bmatrix} \tag{5}$$

$$\begin{Bmatrix} \varepsilon_{xx} \\ \varepsilon_{yy} \\ \varepsilon_{xy} \end{Bmatrix} = \begin{bmatrix} \langle \varphi_x \rangle & 0 \\ 0 & \langle \varphi_y \rangle \\ \langle \varphi_y \rangle & \langle \varphi_x \rangle \end{bmatrix} \begin{Bmatrix} u_1 \\ \vdots \\ u_4 \\ v_1 \\ \vdots \\ v_4 \end{Bmatrix} = [B]\{u\} \tag{6}$$

where: $\langle \varphi_x \rangle = \langle \varphi_{1,x} \ldots \varphi_{4,x} \rangle$ etc.

The element stiffness derives from the expression minimizing the potential energy of the system:

$$\delta \text{ (potential energy)} = 0 \tag{7}$$

$$\sum_{i=1}^{\text{NEL}} \delta(\{P\}_i^T\{u\} - \tfrac{1}{2}\int_{v_i} \{\varepsilon\}^T[C]\{\varepsilon\}\,dv) = 0 \tag{8}$$

$$\begin{aligned}\{P\}_i &= \int_{v_i} [B]^T[C][B]\{u\}\,dv \\ &= [K]_i\{u\}\end{aligned} \tag{9}$$

$$[K]_i = \int_{v_i} [B]^T[C][B]\,dv \tag{10}$$

where:

$\{P\}_i$ = generalized nodal forces (element $[i]$)

$[C]$ = matrix of elastic constants

$[K]_i$ = element stiffness (element $[i]$)

NEL = number of elements.

The stiffness matrix, $[K]$, in equation (10) can be seen to be a linear function of the material constants, C_{ij}. It is possible, therefore, to express equation (9) in an alternative form by reordering the variables:

$$\{P\} = [\bar{K}(u)]\{C\} \tag{11}$$

where:

$[\bar{K}]$ = reformulated element stiffness

and:

$$C_1 = C_{11} \qquad C_2 = C_{12} \qquad C_3 = C_{13}$$
$$C_4 = C_{22} \qquad C_5 = C_{23} \qquad C_6 = C_{33}.$$

The "direct stiffness" assembly of element equations leads to two equivalent stiffness expressions for the solid configuration.

$$\begin{aligned}\{R\} &= \underset{N\times N}{[K]}\ \{r\} \qquad \text{(a)} \\ \{R\},\{r\} &= \text{global load and displacement} \\ \{R\} &= \underset{N\times 6}{[\bar{K}(r)]}\{C\} \qquad \text{(b).}\end{aligned} \tag{12}$$

The first equation, equation (12a), expresses the nodal equilibrium in terms of displacement unknowns, while the second, equation (12b), expresses the equilibrium in terms of material unknowns.

Equation (12b) is non-square, and must be solved in terms of least-squares:

$$\{C\} = [[\bar{K}]^T[\bar{K}]]^{-1}[\bar{K}]\{R\}. \tag{13}$$

The matrix, $\{C\}$, therefore, represents a form of mathematical "best fit" approximation to the material constants which is based upon a measured (or approximate) set of nodal displacements, $\{r_a\} \cong \{r\}$.

An alternative approach to equation (12b) is obtained by splitting the matrix $[C_{ij}]$ into six positive-definite component matrices:

$$[C_{ij}] = \alpha_1[C_{ij}]^{(1)} + \alpha_2[C_{ij}]^{(2)} + \ldots + \alpha_6[C_{ij}]^{(6)} \tag{14}$$

giving the equivalent-least squares solution:

$$\{R\} = [\alpha_1[K]^{(1)} + \alpha_2[K]^{(2)} + \ldots + \alpha_6[K]^{(6)}]\{r\} \tag{15}$$

$$\{R\} = [\alpha_1\{R\}^{(1)} + \ldots + \alpha_6\{R\}^{(6)}] = [\bar{R}]\{\alpha\} \tag{16}$$

$$\{\alpha\} = [[\bar{R}]^T[\bar{R}]]^{-1}[\bar{R}]^T\{R\}. \tag{17}$$

Experimentally, the determination of C_{ij} is obtained from equation (13) or equations (14), (17) by measuring deflections at each node point and computing either $[\bar{K}]$ or $[\bar{R}]$. Any solution, however, must be coupled with the least-squares fit of the experimental data, which can be numerically sensitive.

In terms of computational ill-conditioning, the freedom of choice in equation (15) of the component matrices $[C_{ij}]^{(i)}$ permits the matrix $[\bar{R}]$ to be better conditioned than $[\bar{K}]$. A choice of $[C_{ij}]^{(i)}$ such that $\{R\}^{(i)^T} \cdot \{R\}^{(j)} = 0$ and $\{R\}^{(i)^T} \cdot \{R\}^{(i)} \neq 0$ provides an ideally conditioned system of equations.

A computational problem also arises when few non-zero components enter the matrix $\{R\}$, i.e. whenever a small number of node forces are present. Then, small displacement errors in $\{r_a\}$ can cause the sum of the squares of the residuals,

$$\{E\} = \{R\} - [\bar{K}]\{C\} \tag{18}$$

to be of the same order as the sum of the squares of the node forces, i.e. $\{E\}^T\{E\} \cong \{R\}^T\{R\}$. In such a case, the solution, equations (13), (17), produces a degenerate solution:

$$\{C\} \text{ or } \{\alpha\} \cong \{0\}. \tag{19}$$

Figure 3 illustrates the sensitivity of the solution as the norm of $\{E\}$, designated by $\|E\|$, approaches the norm of $\{R\}$, designated by $\|R\|$.

The two basic equations, equations (13), (17), are directly applicable to experimental programs in which point displacements are recorded as data. Both equations, however, require data to be recorded at *each* node point, and are subject to both an excessively large number of measurements and to the accompanying sensitivity of the least-squares solution [see equations (18), (19)]. More importantly, the computation of $|\bar{K}|$ and $|\bar{R}|$ will become increasingly sensitive to measurement errors as the mesh size is refined. The increased sensitivity reflects the necessity of computing differences between nearly equal displacements.

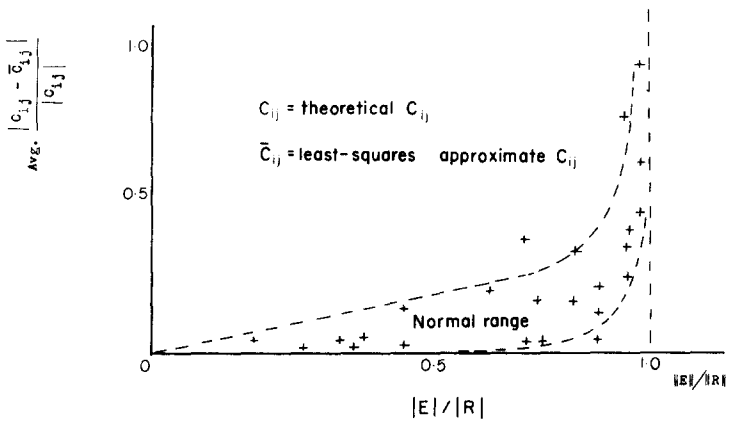

FIG. 3. Least-squares sensitivity.

To eliminate the above sensitivity, an iterative scheme can be employed. Undesirable nodal points† are "condensed" from the solution using a combination of equation (12a) and equation (12b). The matrix condensation:

$$\left\{\begin{matrix} R \\ \cdots \\ Q \end{matrix}\right\} = \left[\begin{matrix} K_{11} & \vdots & K_{12} \\ \cdots & \vdots & \cdots \\ K_{21} & \vdots & K_{22} \end{matrix}\right] \left\{\begin{matrix} r \\ \cdots \\ q \end{matrix}\right\} \begin{matrix} (M) \\ (N-M) \end{matrix} \tag{20}$$

$$\{R - K_{12}K_{22}^{-1}Q\} = [K_{11} - K_{12}K_{22}^{-1}K_{21}]\{r\} \tag{21}$$
$$(M \times M)$$

proceeds directly from equation (12a). (M) defines the number of data points remaining after $(N-M)$ points have been condensed.‡

Condensation implies a partial solution for $\{q\}$ in terms of $\{r\}$, and therefore, requires some knowledge of the material properties. Such a solution must be approached iteratively, in which $[K_{12}]$ and $[K_{22}]$ are expressed in terms of an estimated material law, $[\bar{C}_{ij}]$. $[K_{11}]$ and $[K_{21}]$ are then reformulated as in equation (12b) to give:

$$\{R - K_{12}K_{22}^{-1}Q\} = [\bar{K}_{11} - K_{12}K_{22}^{-1}\bar{K}_{21}]\{C\}. \tag{22}$$
$$M \times 6$$

The recursive use of equation (22) leads to a cyclic re-estimation of $\bar{C}_{ij}^{(i)}$ and recalculation of $\bar{C}_{ij}^{(i+1)}$ at each step. When $\bar{C}_{ij}^{(i)}$ and $\bar{C}_{ij}^{(i+1)}$ coincide, the iteration is complete.

The question of convergence of equation (22) as an iterative solution is problematic, since the convergence is a function of several parameters: (1) the type of boundary-value problem, (2) the number of points retained, (3) the choice of points retained, (4) the relative number of points condensed to points retained, and (5) the number of different stress states in the specimen.

A computer investigation of convergence was conducted to estimate convergence properties on the following bases: (1) random errors in $\{r_a\}$ were limited to $\|E\| \leq \frac{1}{2}\|R\|$,

† Points for which no measurements are recorded.

‡ For plane stress $M \geq 6$.

(2) all boundary-value problems yielded more than one distinct strain state, and (3) comparisons were restricted to the relative number of points retained in the solution. As a results of the investigation, automatic convergence appeared assured whenever:

$$100 \times \frac{|C_{ij}^{\infty} - C_{ij}^{1}|}{|C_{ij}^{\infty}|} \leq 10 \text{ per cent} \qquad \text{(a)}\dagger$$

$$\|K_{11}\| \geq \|K_{12}K_{22}^{-1}K_{21}\| \qquad \text{(b)} \qquad (23)$$

$$\{R\} \text{ fully populated} \qquad \text{(c)}$$

irrespective of the choice of remaining data points.‡

Equation (23a) is a prohibitive requirement, since it demands that the initial guess be within 10 per cent of the true solution (for each of the components in $[C_{ij}]$). It is possible, however, to carefully select the measured data points such that equation (23a) is extended to:

$$100 \times \frac{|C_{ij}^{\infty} - C_{ij}^{1}|}{|C_{ij}^{\infty}|} \leq 50 \text{ per cent.} \qquad (24)$$

The selection process requires prior analysis of the boundary-value problem to determine points which are sensitive to changes in the material constants. It is distinctly advantageous to select data points such that an equal number of points are sensitive to changes in each of the material constants.

The convergence can be aided by an initial set of iterations using a coarse mesh—defined as one in which the stress state will be approximately 10 per cent in error. Since iteration time increases as the square of the mesh refinement (square of the band width), many more iterations can be carried out in comparable time on a given coarse mesh. A reasonable coarse mesh was found to be one-half as refined as the mesh required to give the desired "final" material constants. Figure 4 shows the rate of convergence of the iteration when different coarse mesh schemes are applied.

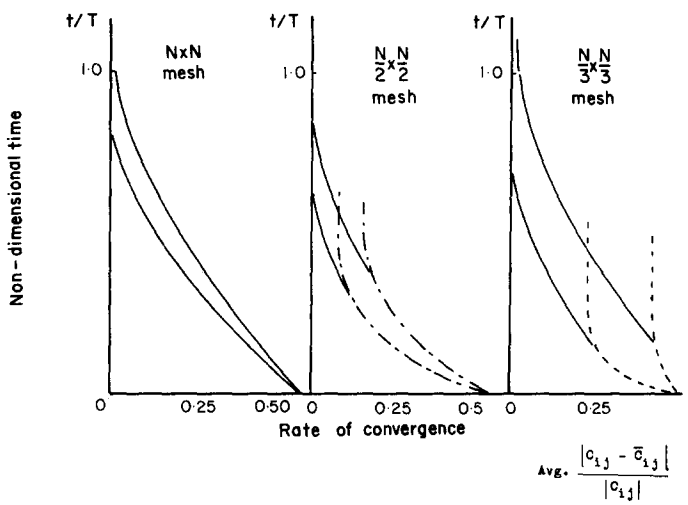

FIG. 4.

† C_{ij}^{n} = nth iterative refinement of the initial material estimate C_{ij}^{0}.

‡ So long as the remaining data points did not yield a singular set of equations.

NONLINEAR ELASTIC MATERIALS [5, 7]

Equations (14), (18) are applicable to the characterization of nonlinear elastic materials, provided the nonlinearity can be expressed as a linear combination of nonlinear functions. A hyperelastic formulation can be used to represent the strain energy in polynomial form:

$$\sum_{i=1}^{\text{NEL}} \delta[P_i^T u - \psi_i(I_1 I_2 I_3)] = 0 \qquad I_1 = \varepsilon_{kk} \qquad I_2 = \varepsilon_{ij}\varepsilon_{ij} \qquad I_3 = \varepsilon_{ij}\varepsilon_{ik}\varepsilon_{jk} \tag{25}$$

where ψ is an isotropic strain energy function:

$$\begin{aligned} \psi &= C_1 I_1^2 + C_2 I_2 + C_3 I_1^3 + C_4 I_1 I_2 + C_5 I_3 + C_6 I_1^4 + \dots \\ C_i &= \text{material constants.} \end{aligned} \tag{26}$$

Equations (25), (26) are functions of the invariants of the strain tensor,

$$\begin{aligned} \delta\psi &= \frac{\partial \psi}{\partial \varepsilon_{ij}} \delta\varepsilon_{ij} = \sigma_{ij}\delta\varepsilon_{ij} \\ &= \left(\frac{\partial \psi}{\partial I_1}\frac{\partial I_1}{\partial \varepsilon_{ij}} + \frac{\partial \psi}{\partial I_2}\frac{\partial I_2}{\partial \varepsilon_{ij}} + \frac{\partial \psi}{\partial I_3}\frac{\partial I_3}{\partial \varepsilon_{ij}} \right) \delta\varepsilon_{ij} \\ &= (\Phi_1 \delta_{ij} + \Phi_2 \varepsilon_{ij} + \Phi_3 \varepsilon_{ik}\varepsilon_{jk})\delta\varepsilon_{ij} \end{aligned} \tag{27}$$

in which the strains are written using indicial notation:

$$\begin{aligned} \varepsilon_{ij} &= \tfrac{1}{2}(u_{i,j} + u_{j,i} + \tfrac{1}{2}u_{k,i}u_{k,j}) \\ \varepsilon_{ij} &= \text{Lagrange strain tensor} \\ u_i &= \text{deflection in direction } X_i \\ u_{i,j} &= \partial u_i / \partial x_j. \end{aligned} \tag{28}$$

Strains, and the corresponding finite element equations are developed in indicial form through equations (28), (3) and (5):

$$\begin{bmatrix} u_{1,1} & u_{1,2} \\ u_{2,1} & u_{2,2} \end{bmatrix} = \begin{bmatrix} \langle \varphi_{,x} \rangle \\ \langle \varphi_{,y} \rangle \end{bmatrix} \begin{bmatrix} u_1 & v_1 \\ \vdots & \vdots \\ u_4 & v_4 \end{bmatrix} = [u_{i,j}]. \tag{29}$$

The finite element analytical solution is obtained as the solution to a nonlinear set of equations, equations (25)–(29). Equation (25), however, is specialized to be nonlinear in the displacement gradients only. In a similar fashion to equation (12b), equation (25) can be reformulated in terms of the material constants:

$$\underset{N \times S}{\{R\} = [\bar{K}]} \begin{Bmatrix} C_1 \\ \vdots \\ C_S \end{Bmatrix} \tag{30}$$

S = number of material constants

N = number of nodal points.

The nonlinear nature of equation (25) will prevent any reformulation in terms of equations (14)–(17), and more importantly, will prevent an iterative solution of the type shown in equations (20)–(22). The solution, equation (30), is rarely a one-step process, however, since it is necessary to determine whether or not the material expansion, $\psi = \sum_1^S C_i f_i(I_1 I_2 I_3)$, is sufficiently general to characterize the material over the experimental range of strain, (I_1, I_2, I_3). When the expansion, ψ, is not sufficiently general, it is necessary to fit the polynomial over a subset of the equations in $[\bar{K}]$ representing a localized region of the space (I_1, I_2, I_3).

The experimental procedure has been investigated [5] for a polyurethane foam specimen. The specimen, shown in Fig. 5, was loaded with six point-loads, using three variations of the load configuration. A total of six experiments was performed, resulting in a combined strain range of approximately:

$$\begin{aligned} -0{\cdot}10 < I_1 < 0{\cdot}31 \\ 0{\cdot}0 < I_2 < 0{\cdot}04 \\ -0{\cdot}001 < I_3 < 0{\cdot}01. \end{aligned} \tag{31}$$

It was determined in that investigation that no polynomial incorporating less than fourth order terms in the strain, ε_{ij}, could represent the foam behavior over the total range of (I_1, I_2, I_3). The procedure failed whenever the polynomial expansion was fit over an

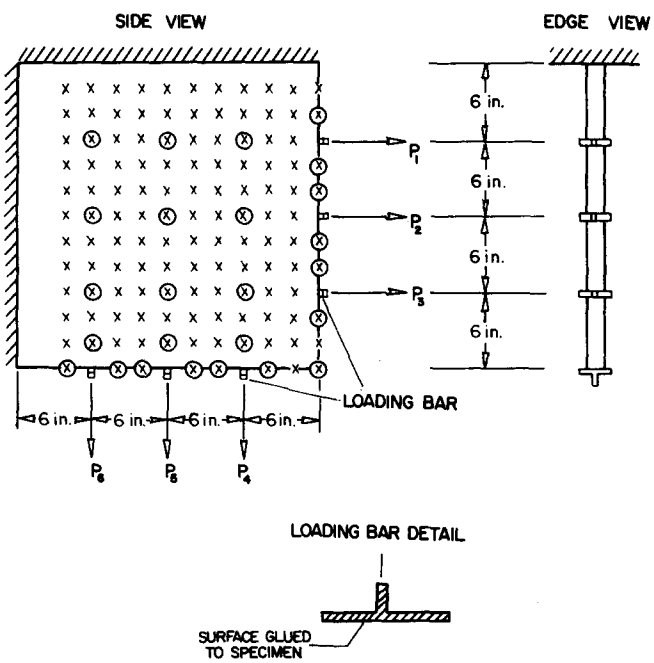

FIG. 5. Polyurethane specimen (tension test). (Reproduced from Ref. [5].)

apparent discontinuity in the stress–strain behavior† and whenever the material exhibited significantly inelastic behavior.‡

A stable least-squares fit was achieved by subdividing the strain range into four subregions:

$$\begin{array}{llll} -0{\cdot}1 < I_1 < 0 & 0 < I_1 < 0{\cdot}04 & 0{\cdot}04 < I_1 < 0{\cdot}09 & 0{\cdot}09 < I_1 < 0{\cdot}31 \\ 0 < I_2 < 0{\cdot}009 & 0 < I_2 < 0{\cdot}005 & 0{\cdot}005 < I_2 < 0{\cdot}012 & 0{\cdot}01 < I_2 < 0{\cdot}04 \\ 0 < I_3 < 0{\cdot}001 & 0 < I_3 < 0{\cdot}0009 & 0{\cdot}001 < I_3 < 0{\cdot}004 & 0{\cdot}004 < I_3 < 0{\cdot}01. \end{array} \quad (32)$$

The piecewise fit for the fourth order expansion (in ε_{ij}) predicted analytically the observed experimental strains to within 20 per cent—in all regions of the specimen. The error was less than $\frac{1}{3}$ the error introduced by a linear least-squares law (quadratic in ε_{ij}). The 20 per cent error reflected measurement errors in the experiment as well as computational errors arising from the discontinuities in the piecewise defined strain energy function.

CONCLUDING REMARKS

A series of computational schemes have been presented for the characterization of elastic solids from statically indeterminate test specimens. The computational schemes require a least-squares "fit" of the experimental data, which in turn, assumes that at least (N) independent equations exist for the determination of (N) material constants. The existence of independent equations becomes fundamental to the choice of experimental specimens, since any homogeneous stress or strain state will yield a singular matrix solution.

An iterative procedure is based on the requirement for a limited number of experimental measurements. The procedure is generally well-suited to experimental investigations, since those data points with high relative measurement error can be eliminated from the analysis. The iterative procedure, however, is not assured of convergence. Additional studies will be required to determine which parameters control the convergence, and which measurement points create the least experimental sensitivity.

The procedure has been applied to the characterization of nonlinear elastic materials, assuming a special power series representation of the strain energy function. In this case, laboratory experiments were performed to demonstrate the method. Approximate material constants were derived, and subsequently used to predict the experimental deformations. Such a comparison limited the test of material constants to those states of strain explicitly contained in the characterization. It is emphasized that any comparison with different ranges of strain constitutes an extrapolation of the results which may not be valid.

REFERENCES

[1] M. J. TURNER, R. W. CLOUGH, H. C. MARTIN and L. TOPP, Stiffness and deflection analysis of complex structures. *J. Aerospace Sci.* **23**, (1956).

[2] C. W. BERT, B. L. MAYBERRY and J. D. RAY, Behavior of Fiber-Reinforced Plastic Laminates Under Uniaxial, Biaxial and Shear Loadings, U.S. Army Materials Testing Laboratory, Fort Eustis, Virginia (1969).

† Flexible polyurethane foam exhibits markedly different tensile and compressive properties—approximating a discontinuity in the stress–strain trace at the origin (zero stress).

‡ Exhibited in the highest region of strain.

[3] E. L. TERRY and S. W. MCCLAREN, Biaxial Stress and Strain Data on High Strength Alloys for Design of Pressurized Components, Chance-Vaught Corp., ASD Technical Document, Wright-Patterson Air Force Base, Ohio (1962).
[4] C. KARNES and L. D. BERTHOLF, Numerical Investigation of Two-Dimensional Axisymmetric Elastic–Plastic Wave Propagation Near the Impact End of Identical 1100-0 Aluminum Bars, *Battelle Colloquium on Inelastic Behavior of Solids*. Battelle Memorial Institute, Ohio (1969).
[5] K. T. KAVANAGH, Finite Element Analysis of Physically and Kinematically Nonlinear Elastic Solids, PhD. Dissertation, University of California, Berkeley (1969).
[6] B. IRONS, Numerical Integration Applied to Finite Elements, *International Symposium on the Use of Digital Computers in Structural Engineering* (1966).
[7] J. T. ODEN, Numerical formulation of nonlinear elasticity problems. *Proc. Am. Soc. civ. Engrs* **93**, (1967).

(*Received* 18 *November* 1969; *revised* 16 *April* 1970)

Абстракт—С целью установления основы программы экспериментального исследования композиционных и некомпозиционных материялов, используется изложение конечного элемента, касающееся теоремы минимума потенциальной энергии. Универсальность вариационного способа позваляет включить в экспериментальную программу образцы, обладающие произвольной геометрией, при широком разнообразии граничных напряженных и кинематических условий.

Полученная экспериментальная программа использует сравнения между метематическими результатами и экспериментальными измерениями, с целью оценки аналитической точности суммарных приближенных механических описаний.